International Journal of Applied Power Engineering (IJAPE)
Vol. 15, No. 2, June 2026, pp. 449~463
ISSN: 2252-8792, DOI: 10.11591/ijape.v15.i2.pp449-463

Transient stability analysis of a new proposed hybrid PV-WTG microgrid for Tinghir power distribution

Hicham Stitou, Mohamed Amine Atillah, Abdelghani Boudaoud, Mounaim Aqil
Engineering and Applied Physics Team (EAPT), Superior School of Technology, Sultan Moulay Slimane University, Beni Mellal, Morocco

Article Info

Article history:

Received Jan 23, 2025
Revised Dec 5, 2025
Accepted Jan 9, 2026

Keywords:

CCT
Critical clearing time
ETAP software
Hybrid systems
Microgrid
Power systems
Transient stability

ABSTRACT

This work focuses on the transient stability of a hybrid photovoltaic and wind turbine generator (PV-WTG) system at the Tinghir 225/60/11 kV substation in Morocco. Results were obtained by evaluating the effects of the proposed configuration on power angle, frequency, voltage, and fault-clearing times in the system. The study examined key disturbances, including abrupt loss of renewable energy and major electrical faults. Analysis using ETAP demonstrated a power angle change of -55 degrees, 20 degrees greater than the normal operating point, which can be caused by the loss of PV and approaches the IEEE Std 421.5 stability limit. The maximum voltage variation was 6.1% for the PV and 2.7% for the WTG, exceeding the IEC 60034-1 limits of ±5%. Another major finding of this analysis was that WTG loss induces frequency swings of 0.8 Hz and requires 10 to 15 seconds for recovery, indicating that low-inertia systems have insufficient inertia to return to steady state quickly. Therefore, the study demonstrates that adaptive control approaches must be used to achieve stable operation of hybrid connected microgrids. Using the time domain simulation (TDS) process, we calculated the critical clearing time (CCT) of 155 ms for 3-phase faults and 464 ms for line-to-ground faults, all of which are within the CCT limit set by IEEE Std 3002.2, and this confirms the necessity of urgent clearing of faults to maintain transient stability and demonstrates the need for fast protection and adaptive control in low-inertia systems, which is of particular concern in rural grids.

Corresponding Author:

Hicham Stitou
Engineering and Applied Physics Team (EAPT), Superior School of Technology
Sultan Moulay Slimane University
Beni Mellal, Morocco
Email: hicham.stitou@usms.ma

1. INTRODUCTION

With rising energy consumption, Morocco will have to significantly expand and upgrade its electrical networks to meet future and current energy demand requirements. To help meet these power needs, electrical engineers will need to conduct an extensive analysis of the network's performance to ensure the network continues to operate efficiently and reliably under normal conditions and during possible disturbances [1], [2]. Power system stability plays an important role in making sure electrical networks stay stable because they are dynamic systems consisting of continuous interactions between generators, loads, and transmission facilities [3]. Instabilities created by any aspect of these complex systems can lead to a chain reaction of failures and, eventually, the loss of service. Therefore, stability analysis is an important area in maintaining a reliable source of energy.

The complexity involved in integrating renewable energy sources (RES) into an existing power grid increases with added levels of penetration. In addition to the potential environmental benefits of RES, hybrid renewable systems can pose challenges on the technical side, such as difficulties regulating voltage, as well as concerns with the stability of the grid due to the variable nature of renewable energy generation [4], [5]. As documented in [6], several advanced techniques to address these challenges were proposed. A major distinction between classic power generation and RES lies in their operational characteristics; traditional generators provide inherent system inertia, while RES typically rely on power electronic converters that do not have this property to help stabilize the system [7], [8].

The literature states that electrical grid stability can be classified into three basic types depending on the type of system impact and how long that impact will last on the electrical grid [9]–[11]. Steady-state stability refers to how well a power system will continue to work under slow but significant changes in load or generation over extended periods. Dynamic stability describes the electrical grid's ability to respond to steady state oscillations and electrical dynamic interactions between generators and loads over a period of many seconds to many minutes. Transient stability may be the most critical type of electrical grid stability because it assesses the grid's performance, especially with respect to maintaining generator synchronization, during and shortly after very large impact events such as a generator failure or fault on the grid, typically measured in tens of milliseconds to a few seconds.

Research approaches for analyzing transient stability in modern power systems following sudden, large disturbances can be categorized into five methodological frameworks [12]. Simulation methods employ step-by-step integration techniques to capture nonlinear system dynamics, providing intuitive results but often at high computational cost [13], [14]. While direct techniques of Lyapunov's theory of stability provide important information regarding stability margins, they also have the added difficulty of being unable to formulate a suitable energy function for a complex system [15]. On the other hand, methods based on data and machine learning (ML) use analytics and ML implementations; however do not provide much insight into how disturbances affect system performance [16]. Furthermore, analytical approaches develop accurate mathematical approximations but can be very difficult to utilize in a highly nonlinear system's behaviors [17]. Hybrid methods apply a combination of techniques to generate new solutions; however, they will also embrace the limitations of their constituent parts and require continuing development [18]. Transient stability analysis methodologies have progressed substantially; however, they still have significant voids in the literature. In particular, the following areas have not received adequate research attention. First, the effect of combined use of photovoltaic and wind generation on the transient stability of distribution networks, especially in developing economies, countries as Morocco; second, the analysis of CCTs in hybrid renewable systems for different fault modes; third, the lack of actual case studies using real network data from operational substations.

To fill in these gaps, we have created a model for the Tinghir Substation's (225/60/11 kV) power supply using actual operating data provided by SPIE Maroc, an industrial and tertiary electricity specialist. Based on this data, we have designed and created a new hybrid PV-WTG microgrid that is connected to the Tinghir distribution network, and we have modeled this new system with ETAP software. The primary contribution of this research is that we evaluated the influence of the photovoltaic (PV) and wind turbine generator (WTG) integration on transient stability based on simulations performed under different cases. These simulation cases included the loss of renewable generation at various random times and three-phase and line-to-ground faults occurring at different bus locations within the hybrid system.

The remainder of this paper is structured as follows: i) Section 2 will describe the simulation methodology and the hybrid system model, ii) Section 3 will present the results of transient stability simulations under different fault scenarios, and iii) Section 4 will conclude the paper and outline promising directions for future research in this domain.

2. METHOD

2.1. Design and operational parameters of the 225/60/11 kV Tinghir Substation

Tinghir Substation is an open-air facility featuring extra-high, high, and medium voltage equipment. It has two incoming feeders, two outgoing feeders, and a transformer that delivers 60 kV to the towns of Kalaat Megouna and Tinghir in Morocco's Drâa-afilalet region. To ensure continuity of service, the substation is configured to be a dual supply system [19].

The substation equipment for extra high voltage (EHV 225 kV), HV (high voltage 60 kV), and medium-to-low voltage (MV-LV 11 kV) includes: The 225 kV system is composed of two identical departures (Ouarzazate and Er-Rachidia), each with a 245 kV capacitive voltage transformer, current transformer, single-wave circuit breaker, three-pole circuit breaker, earthing and non-earthing isolating switches, a 225 kV transfer section, a 225 kV busbar, and two 225/60/11 kV transformer sections. The 60 kV

system is composed of two 225/60 kV transformer sections, each equipped with three 72.5 kV measurement units, a three-pole circuit breaker, and a three-pole non-earthing isolating switch.

2.2. Single-line diagram and configurations of the proposed PV-WTG hybrid microgrid

The implemented single-line diagram (SLD) of the 225/60/11 kV Tinghir Substation, using ETAP software, is shown in Figure 1. Whereas Figure 2 illustrates the SLD of the proposed PV-WTG hybrid microgrid connected to the power distribution network in Tinghir. The system integrates renewable sources, loads, transformers, and buses. The system's primary 11 kV grid connection feeds power through transformer Tn1 (10 MVA) and transformer Tn2 (10 MVA), which step down the voltage to supply Bus_DR and other network sections. Transformer Tn3 (350 kVA) further reduces voltage from the wind generation line, Bus_Wind (11 kV), to Bus_L1 (0.38 kV) for local distribution.

Key buses organize power flow throughout the network. Bus_grid (11 kV) connects directly to the main grid, powering Load_11grid (1 kVA) and feeding into other areas. Bus_DR (0.38 kV) links to Bus_PVA, which supports three photovoltaic arrays (PVA_N1, PVA_N2, and PVA_N3). Bus_Wind (11 kV) collects power from the wind turbine generator (250 kW) and interfaces with other buses. Bus_MTr (0.38 kV) supplies industrial loads and a 75 kW motor (Mtr_1), with additional loads like Lump_L3 (100 kVA) and Lump_L4 (200 kVA). The network includes multiple renewable sources: photovoltaic arrays, a wind turbine, and a hydro generator (Gen_Hydro1, 200 kW), which diversifies power input. Protection devices, including circuit breakers, are positioned across the system to ensure safety, with grounding points maintaining stable voltage references.

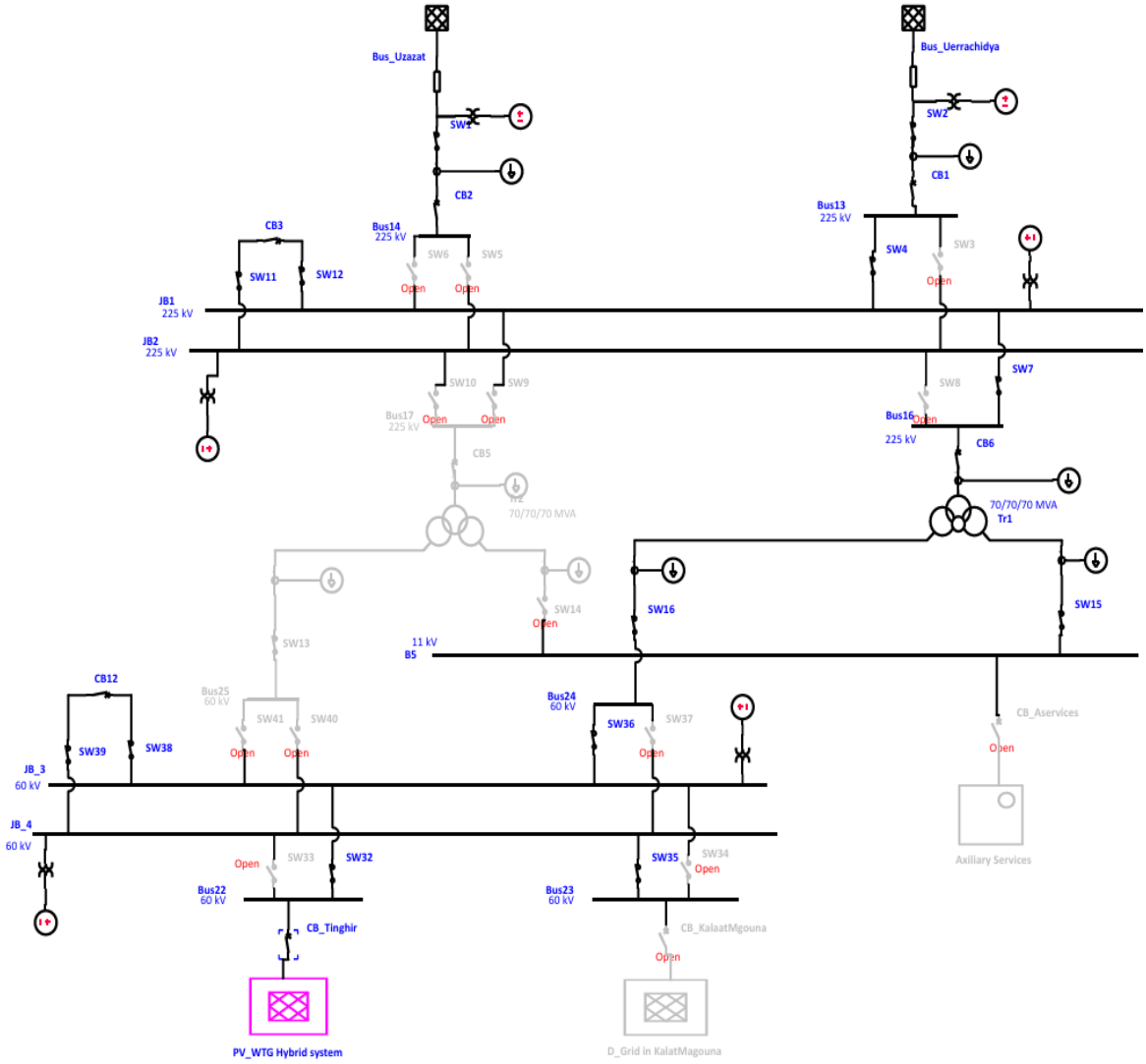

Figure 1. SLD of 225/60/11 kV substation in Tinghir

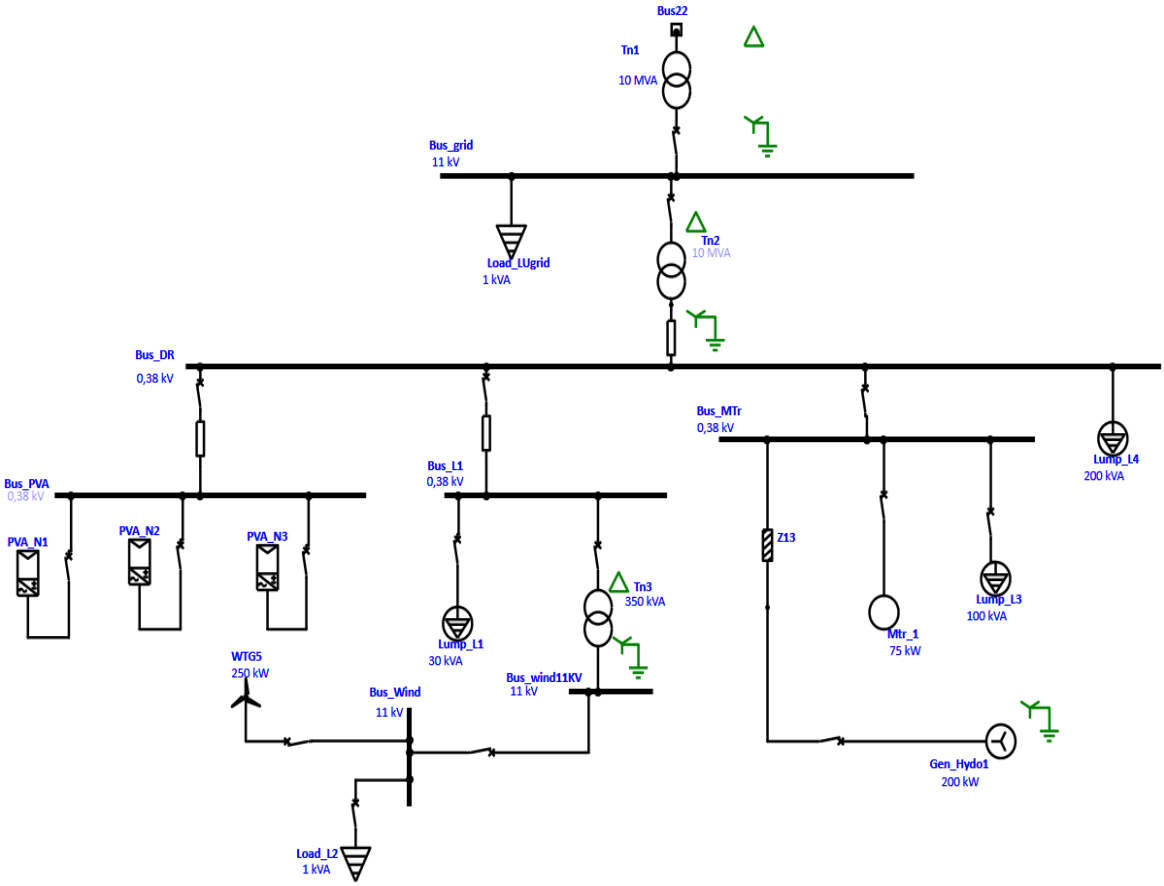

Figure 2. The proposed PV-WTG hybrid system for Tinghir distribution grid

2.2.1. Hydro generator configuration

The hydro generator in the hybrid PV-WTG microgrid operates in swing mode, with its simulation data provided in Table 1. The AC1C dynamic model, part of IEEE standards, simulates static excitation systems with feedback control for synchronous generators in power systems [20]. The AC1C dynamic model is used in simulation.

Table 1. Hydro generator configuration

	Static model	Exciter dynamic model
Rating	200 kW 0.38 kV	AC1C
Impedance	X_d"=19	
Inertia	WR^2=114.4, H=6	

2.2.2. PV array system configuration

The PV system used to simulate the hybrid system consists of three groups of photovoltaic arrays. Under uniform irradiation of 1000 W/m², the total power output of the PV system is approximately 608 kW. Figure 3 presents the electrical characteristics of the photovoltaic panel, including power-voltage and current-voltage curves, which were considered in the design of the PV array system. The detailed specifications of the PV arrays are provided in Table 2. The inverter data configuration, including DC ratings, efficiency, and AC ratings, is given in Table 3.

Table 2. Specifications of the PV system used for simulation

PV array	Panel model	P/panel (W)	Panels in series	Panels in parallel	P total (kW)
PVA_N1	Suniva, ART245-60-3-1,	239.7	22	44	232
PVA_N2	Mono-crystalline, 60 cells,	239.7	22	44	232
PVA_N3		239.7	20	30	143.8

Table 3. Specifications and rated capacity of the inverter

Category	Specification	Rating	Unit
DC characteristics	Power/voltage ratio	232/0.674	kW/kV
	Maximum voltage	110	p.u.
	Minimum voltage	0	p.u.
AC characteristics	Apparent power	209	kVA
	Operating voltage	0.38	kV
	Power factor range	80-100	p.u.
Performance	System efficiency	90	p.u.
Operating range	Voltage tolerance	90-110	p.u.

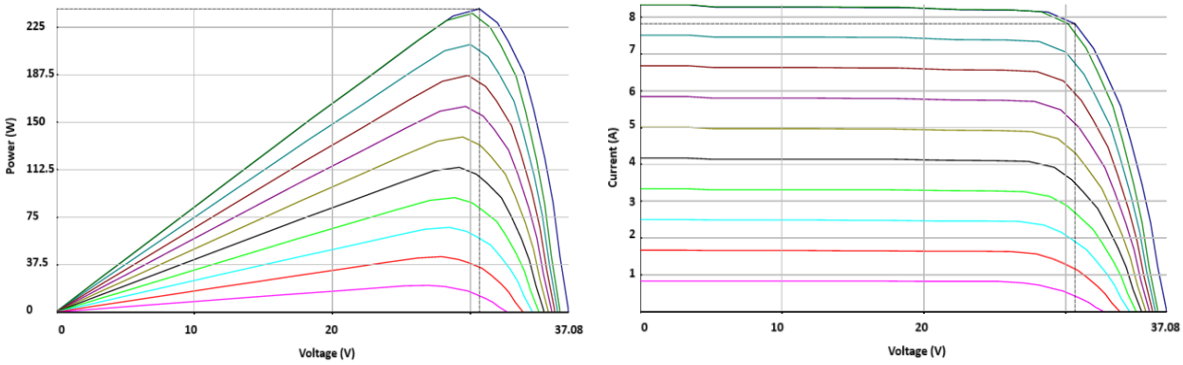

(a) (b)

Figure 3. Electrical characteristics of the PV panel at different irradiation levels: (a) P-V and (b) I-V curves

2.2.3. Wind turbine generator configuration

The wind turbine generator (WTG) modeled in this study is a Type 2 (squirrel-cage induction generator) system with a rated voltage of 11 kV. Key aerodynamic parameters, as configured in ETAP's interface editor, shown in Figure 4, include a cut-in speed of 4 m/s, a cut-out speed of 25 m/s, and a rotor diameter of 60 meters. The turbine operates at a fixed pitch angle of 1° and a nominal RPM of 15, with air density set to the standard value of 1.225 kg/m³, ensuring a realistic power curve representation under IEC 61400-12-1 wind conditions.

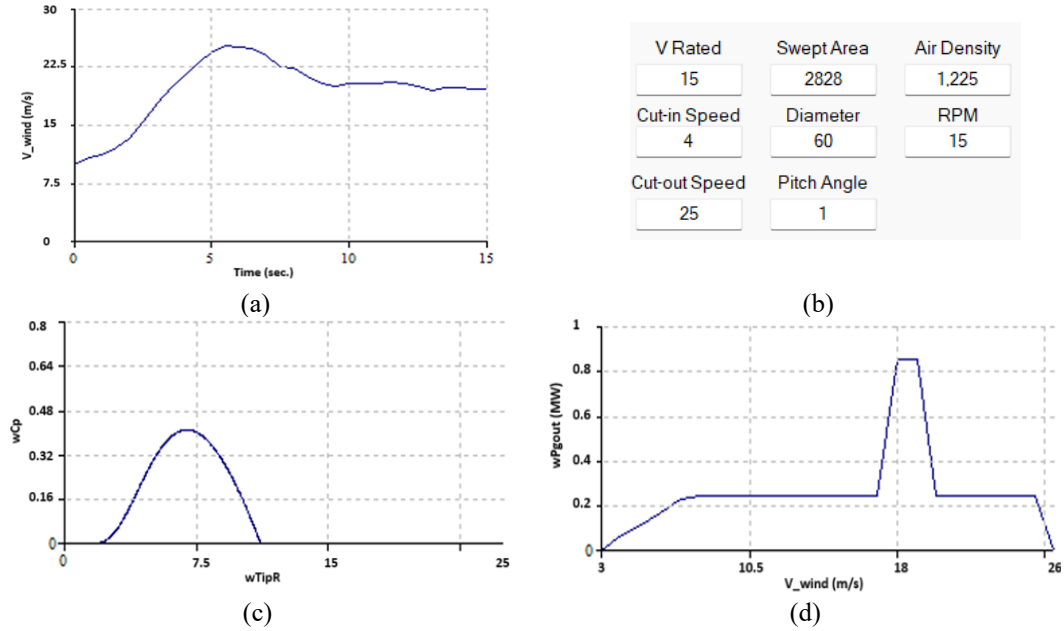

(a) (b) (c) (d)

Figure 4. Wind turbine configuration: (a) wind profile, (b) wind turbine aerodynamic data, (c) wind power coefficient Cp curve, and (d) power curve

2.3. Operational data and environmental assumptions

Operational data was collected in 2024 from "SPIE Maroc". Load profiles exhibited three distinct modes (off-peak, standard, peak), with the WTG loss event occurring under standard loading (1.52 MW). Ambient conditions included a simulated wind speed profile (9→23→18 m/s) and constant simulated irradiation (1000 W/m²). Key assumptions are summarized in Table 4.

Table 4. Summary of key simplifying assumptions

Parameter	Assumption	Limitation
WTG	Instantaneous power response	Neglects pitch delay (~0.5-2 sec.)
PV	Fixed STC (1000 W/m², 25 °C)	Excludes irradiance/thermal variability
Grid	Infinite bus model	Overestimates grid stiffness
Load	Constant during the event	Neglects demand response
Simulation	60-second transient window	Excludes long-term settling

3. RESULTS AND DISCUSSION

To simulate and evaluate the impact of integrating PV and WTG on the transient stability of the hybrid microgrid under study, various scenarios are studied and discussed. This analysis considers events such as the disconnecting of the PV generator and WTG at random times, as well as the occurrence of three-phase (3φ) and line-to-ground (LG) faults on buses near the PV array and near the WTG. The CCT of the faults is determined through extensive testing using the TDS algorithm. Key simulation parameters used for the simulation are summarized in Table 5.

3.1. Transient stability analysis in the proposed PV-WTG hybrid microgrid

For hybrid systems, stability is affected by the intermittency of PV generation, the dynamic characteristics of grid-forming and grid-following inverters, as well as mutual impacts among PV systems and other generators (e.g., hydro generators and wind turbines). Figure 5 shows the flow chart of the simulation adopted for analysis in this work. A specific safety measure obtained from such analysis is the critical clearing time (CCT); the maximum duration that a fault can stay in our system without it losing stability and breaking down.

Table 5. Comprehensive simulation parameters for transient stability analysis

Parameter category	Specific variable	Tested value/range	Unit	Standard reference	Scenario association
System topology	Nominal voltage	225/60/11	kV	IEC 60038	Baseline configuration
	System frequency	50	Hz		
Fault types	Three-phase balanced	Full voltage collapse	-	IEEE Std 3000	Severe stability challenge
	Line-to-ground	80% voltage dip	-		Common rural grid fault
Fault locations	PV inverter bus (bus DR)	0.38 kV	-	IEC 61400-21	Renewable integration impact
	Bus wind	11 kV bus	-		Renewable integration impact
Fault durations	CCT (3φ)	160 (variable step-size)	ms	IEEE 1547	Protection coordination limit
	CCT (LG)	472 (variable step-size)	ms		
Protection settings	Overcurrent relay	1.25×Inom, t=156ms	-	IEC 60255	Primary protection
	Underfrequency relay	58.8 Hz, t=500ms	-		Islanding prevention
Stability thresholds	Voltage deviation	+10%/-15%	p.u.	EN 50160	Power quality compliance
	Frequency deviation	±1 Hz	Hz		

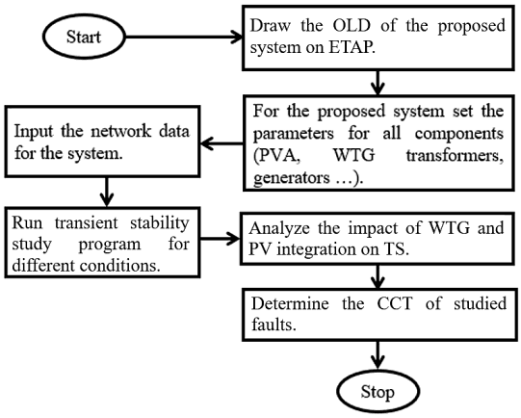

Figure 5. Process to perform transient stability analysis using ETAP software

3.1.1. Process for estimating CCT

CCT is determined through simulation by incrementally increasing the fault clearance time (FCT) until the system transitions to an unstable state. For the studied cases, the TDS algorithm, illustrated in Figure 6, is employed to determine the CCT value [21], [22]. This method provides detailed time-domain responses of system variables, can handle complex, nonlinear system dynamics, and is suitable for all types of power systems, including large-scale grids.

3.1.2. Case 1: Disconnection of PV array from the hybrid microgrid

The PV generator was taken out of the hybrid system by turning off the circuit breaker (CB_PV) for the PV portion of the system at t = 30 s, and Figure 7 shows how the power angle of the generator reacted to this event. During the first 30 seconds, the power angle steadily decreased from 35° to -50°, with small oscillations, indicating that the generator was operating steadily with the assistance of the PV. The sharp drop in the power angle at the time of disconnecting the PV generator shows that a transient interconnection with the grid occurred at that time due to the loss of the PV output. After the disconnection, during the next 30 seconds, the power angle began to oscillate and finally stabilized at approximately -55° as the generator began to adjust to the increased load. Figure 8 illustrates the response of the generator speed. This parameter varied considerably from its nominal value of 1,500 rpm before stabilizing and returning to nominal speed, at time = 45 s, and after about 15 s.

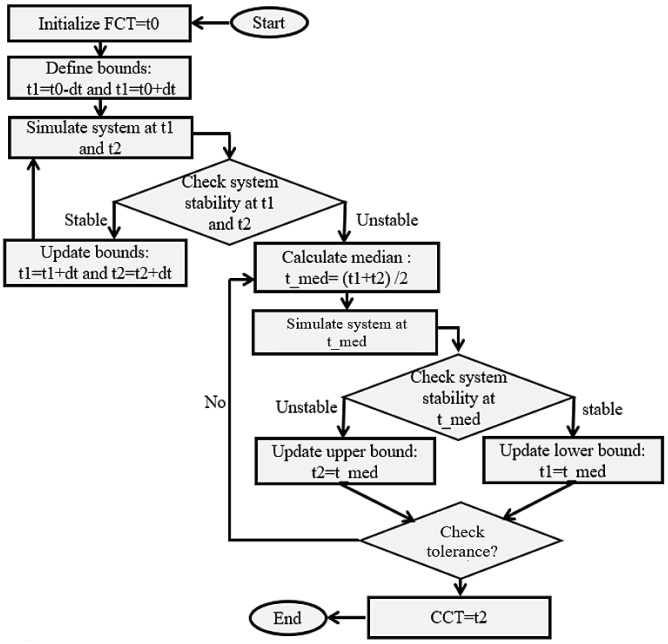

Figure 6. Algorithm for estimating CCT using ETAP software

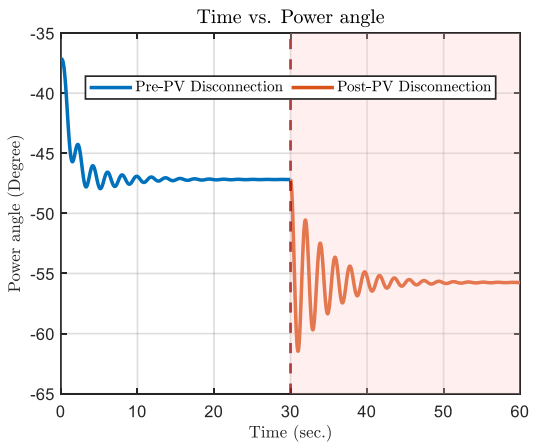

Figure 7. Power angle in degrees

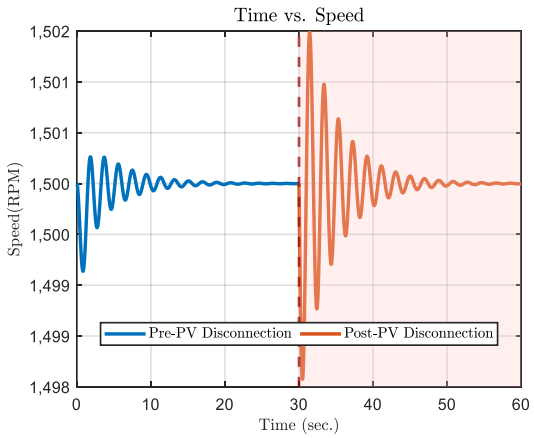

Figure 8. Generator speed in RPM

The impact of PV array disconnection on voltage and frequency stability is analyzed through Bus_DR measurements, with results presented in Figures 9 and 10. As shown in Figure 9, the Bus_DR frequency fluctuates from its nominal value, dropping to 99.88% and peaking at 100.1% after the PV disconnect. These fluctuations reflect the transient disturbance, followed by a recovery process mainly driven by the inertial response of the synchronous generators in the hybrid system. Figure 10 shows the evolution of the Bus_DR voltage. Before the disconnection (0-30 s), the voltage starts at 0.380 kV and gradually decreases with slight oscillations due to the PV contribution. At t = 30 s, there is a sharp voltage drop, indicating a transient response. After disconnection (30-60 s), the voltage stabilizes at around 0.357 kV with small oscillations as the synchronous generator compensates for the power loss.

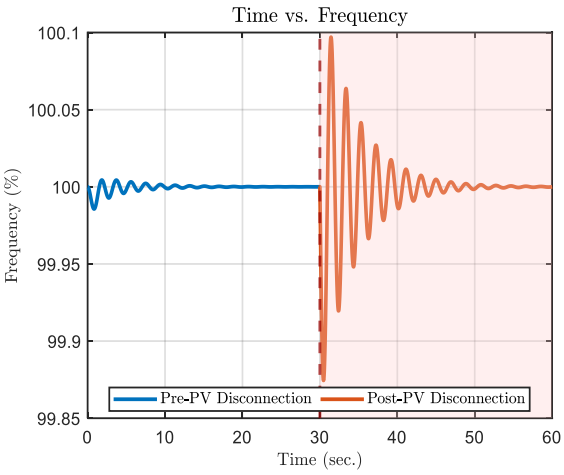

Figure 9. Bus_DR frequency in (%)

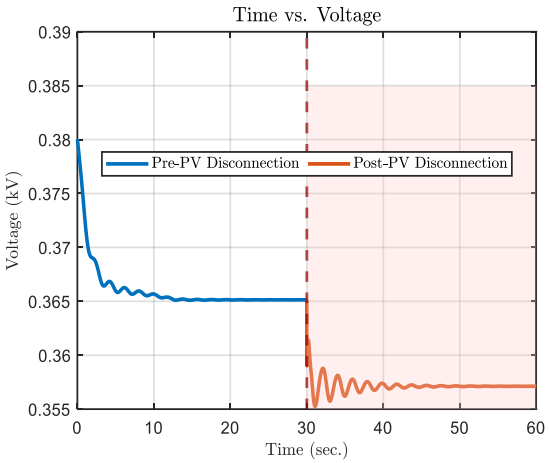

Figure 10. Bus_DR voltage in kV

3.1.3. Case 2: Disconnection of WTG from the hybrid system

This scenario models the shutdown of a WTG at 30 seconds and observes how that affects transient stability using Bus_Wind measurements. The disconnection causes two destabilizing effects, as shown in Figures 11 and 12. First, there is a frequency transient caused by a disturbance from active power imbalance with an initial 0.8 Hz dip and overshoot. The damping mechanism stabilizes the frequency back to its nominal value at 50 seconds. The second effect is due to a reactive power deficit resulting in a 2.7% voltage drop and stabilizing at 10.8 kV, thereby showing how the WTG assists in voltage stabilization.

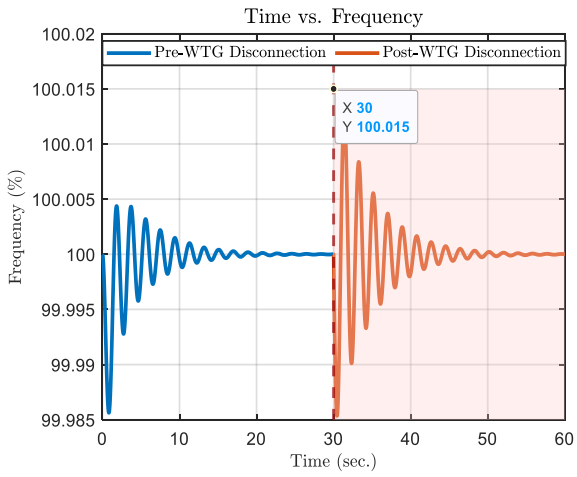

Figure 11. Bus_Wind frequency in %, before and after loss of WTG

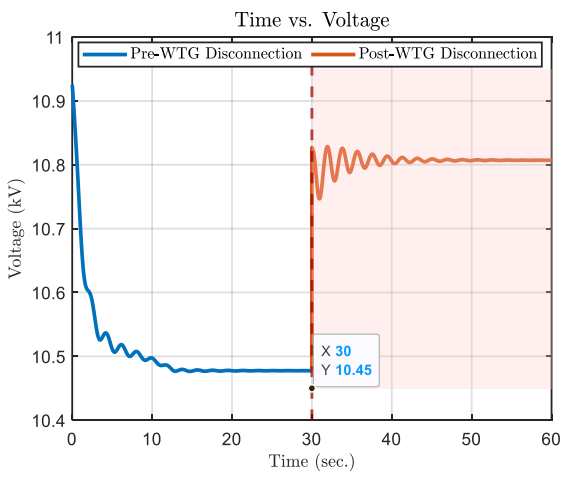

Figure 12. Bus_Wind voltage in kV, before and after loss of WTG

Generator dynamics associated with system stability limits, as identified through electrical current (I) and power angle measurements, demonstrate that grids with a high penetration of renewable energy require responsive control. As can be seen in Figure 13, when a wind turbine generator disconnects, the initial drop of the power angle is significant, followed by sustained oscillations, followed by damping over time until a new steady-state power angle (approx. -50°) becomes established due to the redistribution of power throughout the grid. A similar pattern is observed in the current response shown in Figure 14. When the WTG trips at t = 30 s, the current drops sharply and begins oscillating. These fluctuations gradually subside, stabilizing by t = 45 s at a lower steady-state value that reflects the system's reduced generation capacity following the WTG's disconnection. Together, these responses demonstrate how sudden renewable generation losses can push conventional generators toward their stability limits, a critical consideration for grid operators managing high-penetration renewable systems.

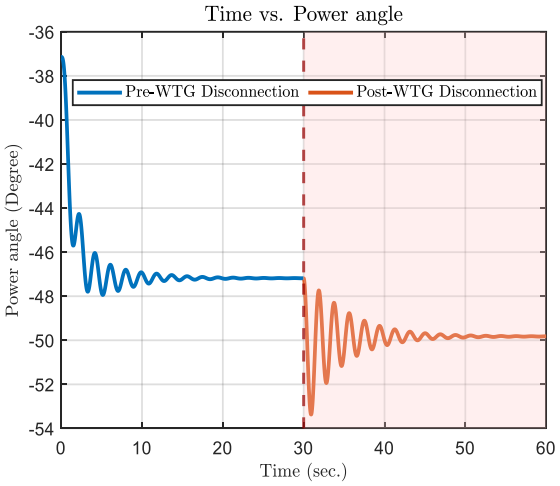

Figure 13. Generator power angle in degrees, before and after loss of WTG

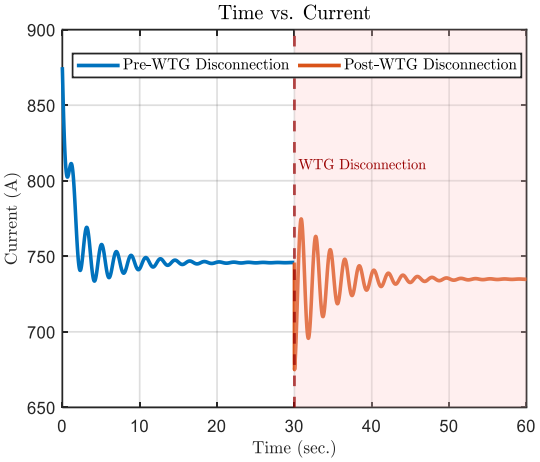

Figure 14. Generator current in A, before and after loss of WTG

3.1.4. Case 3: Three-phase fault near the WTG

This case review, which examines a 3-phase fault occurring at bus wind (near WTG), is triggered when t = 20 s. The clearing time (FCT) is taken as 20.17 seconds to provide a short time/frame for observing transient stability, with the critical clearing time (CCT) being created by reducing the clearing time of the fault until the hydro generator loses synchronism. The power angle of the system generators (in degrees) is shown in Figure 15 for times 0-20 seconds before the fault event, 20 seconds to 20.17 seconds (during the fault event), and 20.17 seconds to 60 seconds (end of the fault). The current spikes that occur during a fault, as demonstrated in Figure 16, exceed 2000 A, which is 2.5 times higher than the operating range of 800 A. This represents a key component for sizing protective equipment as well as determining the equilibrium of the system. In addition to providing a magnitude for the fault occurrence, these spikes also represent the oscillating output of the generator and transient phenomena induced in the power system by the fault. The frequency and damping of this oscillation can be used to validate the performance of protective devices. The progression of the generator power angle (in degrees) is illustrated in Figure 17, and that of the generator current magnitude (in A) in Figure 18 for an instance where the fault was cleared in 155 ms. By evaluating Figures 17 and 18, a critical clearing time (CCT) of 155 ms can be determined.

3.1.5. Case 4: Line-to-ground fault near the PV array

This scenario evaluates the impact of an LG fault occurring near the PV array. The LG fault is created on Bus_DR at 25 s. First, the fault is cleared at t = 26 s. This process will continue, using the proposed algorithm, until the system becomes stable. Figures 19 and 20 illustrate, respectively, the power angle (in degree) and current (in A) of the system's generator before, during, and after the faulty event. Figures 21 and 22 illustrate Bus_DR frequency in (%) and Bus_DR voltage in kV before, during, and after the LG fault. In this condition, and by using the algorithm detailed in Figure 6, the CCT is determined to be 464 ms.

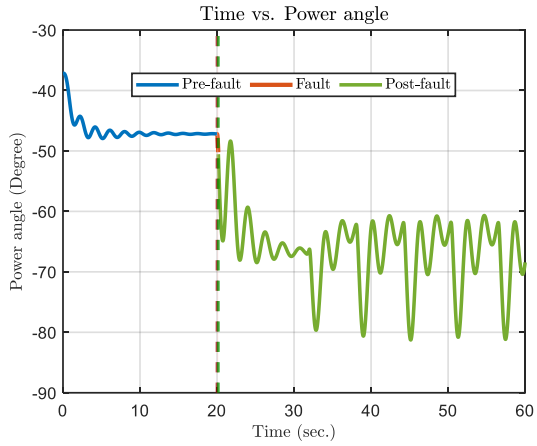

Figure 15. Generator power angle, when FCT is 170 ms

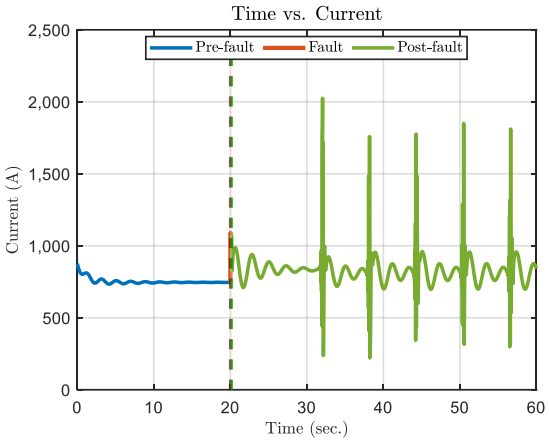

Figure 16. Generator current in A, when FCT is 170 ms

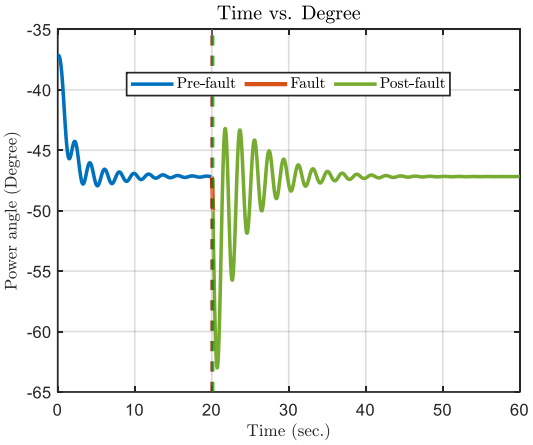

Figure 17. Generator power angle in degrees, when FCT is 155 ms

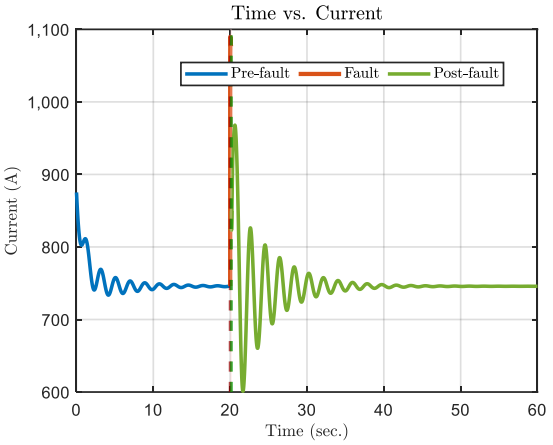

Figure 18. Generator current in A, when FCT is 155 ms

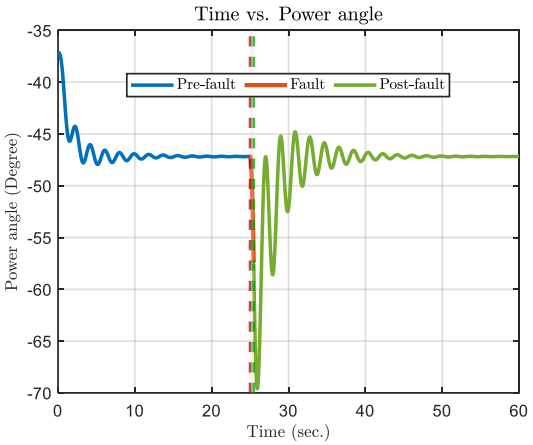

Figure 19. Generator power angle in degrees before, during, and after the LG fault

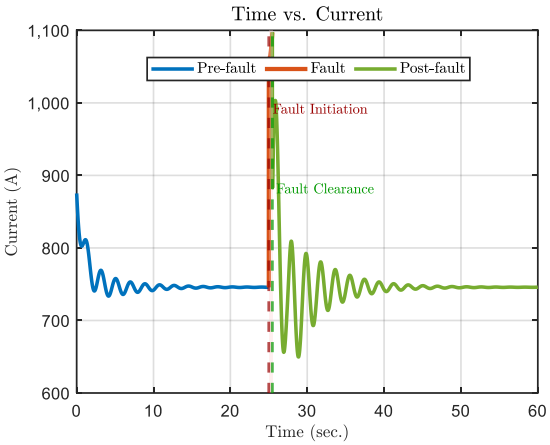

Figure 20. Generator current in A before, during, and after the LG fault

As shown in Figure 21, the Bus_DR frequency fluctuates from its stable state due to the LG fault. Figure 22 shows the Bus_DR voltage profile during the LG fault. Before the fault (0-25 seconds), the voltage remains stable at 0.37 kV. At 25 s, the fault causes a sharp drop in voltage to 0.15 kV. After the fault is cleared at 26 s, the voltage begins to recover, with oscillations reflecting the system's transient response. By 35 seconds, the oscillations dampen, and the voltage stabilizes near its pre-fault level, demonstrating the system's resilience and ability to recover from disturbances.

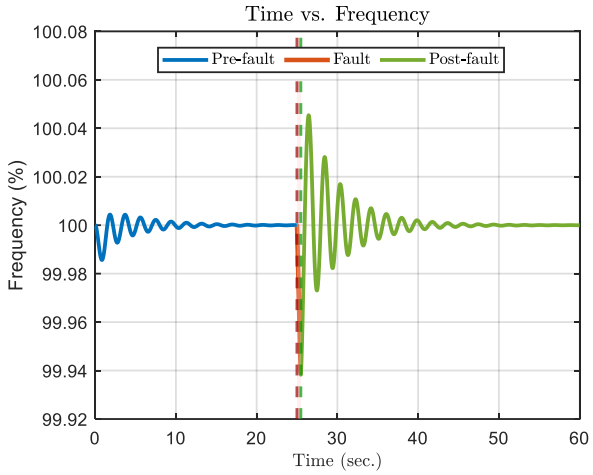

Figure 21. Bus DR frequency in (%) before, during, and after the LG fault

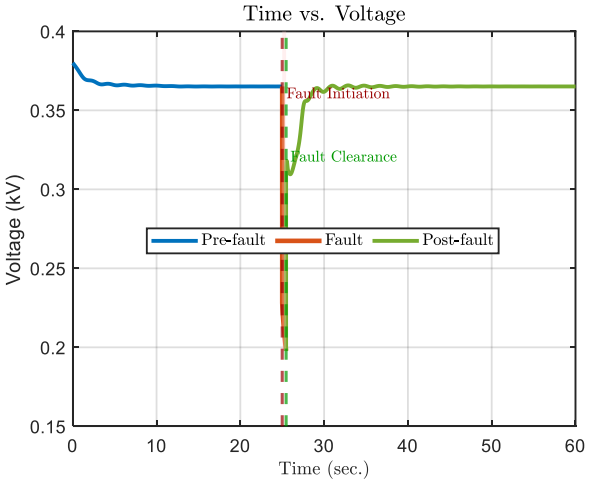

Figure 22. Bus DR voltage in kV before, during, and after the LG fault

3.1.6. Comparative analysis of the results

This study looks at how disconnecting RES like photovoltaic (PV) and wind turbine generators (WTG) from a hybrid power system (HPS) affects the dynamic stability of the system. In four different scenarios for testing, we found that there can be very large voltage swings caused by disconnecting a PV unit (Figure 23) and a decrease in the ability of synchronous generators to support power balance from other generator sources in the HPS. In contrast, when a WTG is disconnected (Figure 24), there is an increase in power angle swings in conjunction with decreases in voltage and frequency, resulting in more oscillation of these parameters because of the combined loss of both active and reactive power. The examples in this section indicate the increasing impact that large quantities of RES technologies will have on the transient stability of HPSs. Therefore, there is an increasing need for developing better and more advanced protection and control strategies to provide continued stability of HPSs while allowing for the integration of RES technologies into hybrid power plants.

The effect of faults on the stability of our PV-WTG system is demonstrated by the data shown in Figures 25 and 26. While the line-to-ground (LG) faults are not as severe as the three-phase faults, LG faults have been shown to decrease the amount of voltage sags produced, thus effectively decreasing the amount of generation capacity from the PV system, whilst causing frequency stability issues associated with lower output-producing PV systems because the system has low inertia. Conversely, the 3-phase fault creates significant disruption in both the power produced by the WTG and the overall stability of the hybrid system, causing a voltage drop immediately while also creating critical frequency variations.

The comparative analysis reveals critical stability thresholds in the hybrid renewable system: generation loss (PV/WTG disconnection) causes manageable voltage and frequency deviations, a 6.1% voltage drop, 0.8 Hz swing. While faults demand fast protection, 3-phase faults require clearing within 155 ms to prevent collapse, whereas LG faults tolerate 464 ms despite severe voltage sags (59% drop). Key metrics highlight the WTG's superior voltage regulation, with a 2.7% drop compared to PV's 6.1%, and the system's reliance on inertial response, achieving frequency recovery within 10 to 15 seconds. The results demonstrate the criticality of using adaptive circuit breaker protection systems (≤100 ms fault response) and grid-forming inverter systems. The measured CCTs meet industry standards, yet they exhibit certain effects that are specific to renewable energy systems: i) The 155 ms 3-phase CCT meets IEEE Std 3002.2-2018's 200 ms limit but reflects tighter PV/WTG grid needs and ii) the 464 ms LG CCT exceeds IEC 60909's typical 30-50% longer allowance due to WTG reactive support and partial power flow.

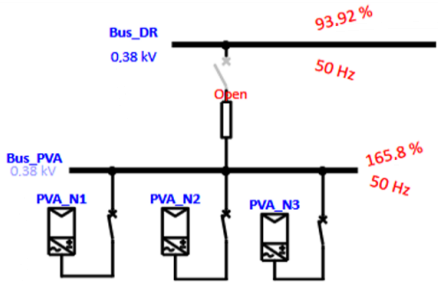

Figure 23. Loss of the PV generator

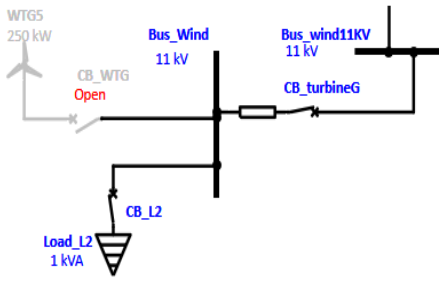

Figure 24. Loss of WTG

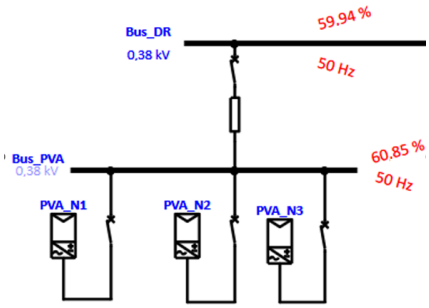

Figure 25. LG fault on bus DR

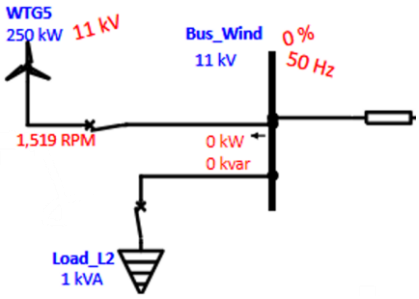

Figure 26. Three-phase fault on bus wind

3.1.7. Comparative results and critical implications

This section contains the results of a comparison of several studies that have been completed regarding transient stability. Table 6 gives a list of transient stability analyses that have been done and lists CCT for each of the configurations used. Generally, the CCT depends on different factors, including the level of power output of the generator, the location and type of fault, the voltages that are present, and the amount of power flow that existed immediately before the disturbance. A comparison of the CCTs for the various studies and their layouts reveals that the Tinghir PV-WTG system demonstrates a greater strength when subjected to LG fault conditions (CCT = 464 ms), surpassing the CCT in the Netherlands grid. The performance of this system is like that of the more robust IEEE 9-bus configurations. This indicates the significant advantages of using WTG solutions in rural areas. However, problems arise due to the low level of inertia associated with the WTG configuration when the system experiences a three-phase fault (CCT = 155 ms). Therefore, transient stability is specific to a given environment, and an adaptable protection scheme must be employed to address the effects of both symmetrical and asymmetrical faults.

Table 6. Transient stability studies for comparison

System type	Research work	CCT (ms)	Case study
PV-WTG system	[23]	242-279	Netherlands grid
Hybrid PV system	[24]	452-465	Modified IEEE 9-bus system
WTG-dominant system	[25]	329-340	Modified IEEE 9-bus + WTG
conventional system	[26]	316-361	IEEE 9 bus system
PV-WTG system (proposed)	This study	155-464	225/60/11 kV Tinghir Substation, Morocco

4. CONCLUSION

This research investigated the transient stability of a hybrid PV-wind system connected to the Tinghir Substation (225/60/11 kV) using ETAP simulation software. The simulation results show that if these renewable sources were suddenly disconnected from the system, the result would be an immediate and severe imbalance in the distribution network, a voltage drop of 6.1% for PV and 2.7% for WTG, which would also result in a frequency excursion of 0.8 Hz. The fault analysis showed that the CCT for three-phase faults was estimated to be 155 ms, and for line-to-ground (LG) faults, it was 464 ms. These findings will be very beneficial in guiding Morocco's move towards renewable energy, because they recommend that ultra-fast relays be used when connecting renewable-heavy networks, recommend that WTG systems with static synchronous compensators be prioritized for the maintenance of voltage stability, and recommend a revision of the national grid codes to acknowledge the loss of inertia experienced by renewable generation plants.

The next phase of this study will focus on the continued integration of renewable energy into Morocco with battery energy storage technologies, and to improve the current mathematical models for transient and dynamic stability through machine learning-based algorithms to optimize the speed and accuracy of CCT estimates. This ongoing work will also explore interregional power lines, enhance resilience to climate-related extreme weather events, and involve local communities in the development of a sustainable energy system that meets Morocco's renewable energy goals.

FUNDING INFORMATION

Authors state no funding involved.

AUTHOR CONTRIBUTIONS STATEMENT

This journal uses the Contributor Roles Taxonomy (CRediT) to recognize individual author contributions, reduce authorship disputes, and facilitate collaboration.

Name of Author	C	M	So	Va	Fo	I	R	D	O	E	Vi	Su	P	Fu
Hicham Stitou	✓	✓	✓	✓		✓			✓	✓				
Mohamed Amine Atillah		✓					✓		✓	✓	✓			
Abdelghani Boudaoud	✓		✓				✓			✓	✓	✓		
Mounaim Aqil	✓	✓		✓		✓				✓		✓		

C : **C**onceptualization
M : **M**ethodology
So : **So**ftware
Va : **Va**lidation
Fo : **Fo**rmal analysis
I : **I**nvestigation
R : **R**esources
D : **D**ata Curation
O : Writing - **O**riginal Draft
E : Writing - Review & **E**diting
Vi : **Vi**sualization
Su : **Su**pervision
P : **P**roject administration
Fu : **Fu**nding acquisition

CONFLICT OF INTEREST STATEMENT

The authors have no conflicts of interest to declare.

DATA AVAILABILITY

The authors confirm that the data supporting the findings of this study are available within the article [and/or its supplementary materials].

REFERENCES

[1] H. Abdi, "Power system analysis using the ETAP software: a comprehensive review," *Research Article Journal of Energy Management and Technology (JEMT)*, vol. 8, p. 250, 2024, doi: 10.22109/jemt.2024.467452.1518.

[2] J. Shair, H. Li, J. Hu, and X. Xie, "Power system stability issues, classifications and research prospects in the context of high-penetration of renewables and power electronics," *Renewable and Sustainable Energy Reviews*, vol. 145, p. 111111, Jul. 2021, doi: 10.1016/j.rser.2021.111111.

[3] N. Hatziargyriou *et al.*, "Definition and classification of power system stability – revisited & extended," *IEEE Transactions on Power Systems*, vol. 36, no. 4, pp. 3271–3281, Jul. 2021, doi: 10.1109/TPWRS.2020.3041774.
[4] A. Ymeri, N. Krasniqi, and R. Shaqiri, "Impact of the wind power plant connection to the Kosovo power system," *IFAC-PapersOnLine*, vol. 55, no. 39, pp. 393–398, 2022, doi: 10.1016/j.ifacol.2022.12.063.
[5] M. Liaqat, T. Alsuwian, A. A. Amin, M. Adnan, and A. Zulfiqar, "Transient stability enhancement in renewable energy integrated multi-microgrids: a comprehensive and critical analysis," *Measurement and Control*, vol. 57, no. 2, pp. 187–207, Feb. 2024, doi: 10.1177/00202940231196193.
[6] J. Hashimoto, T. S. Ustun, M. Suzuki, S. Sugahara, M. Hasegawa, and K. Otani, "Advanced grid integration test platform for increased distributed renewable energy penetration in smart grids," *IEEE Access*, vol. 9, pp. 34040–34053, 2021, doi: 10.1109/ACCESS.2021.3061731.
[7] S. Xia, Q. Zhang, S. T. Hussain, B. Hong, and W. Zou, "Impacts of integration of wind farms on power system transient stability," *Applied Sciences*, vol. 8, no. 8, p. 1289, Aug. 2018, doi: 10.3390/app8081289.
[8] P. Tielens and D. Van Hertem, "The relevance of inertia in power systems," *Renewable and Sustainable Energy Reviews*, vol. 55, pp. 999–1009, Mar. 2016, doi: 10.1016/j.rser.2015.11.016.
[9] A. A. Alsakati, C. A. Vaithilingam, and J. Alnasseir, "Transient stability assessment of IEEE 9-bus system integrated wind farm," *MATEC Web of Conferences*, vol. 335, p. 02006, Jan. 2021, doi: 10.1051/matecconf/202133502006.
[10] E. Munkhchuluun, L. Meegahapola, and A. Vahidnia, "Impact on rotor angle stability with high solar-PV generation in power networks," in *2017 IEEE PES Innovative Smart Grid Technologies Conference Europe (ISGT-Europe)*, Sep. 2017, pp. 1–6, doi: 10.1109/ISGTEurope.2017.8260229.
[11] A. Z. Abass, "Analysis of a gas station hybridization with a solar thermal plant by using ETAP," *International Journal of Applied Power Engineering (IJAPE)*, vol. 10, no. 2, pp. 118–126, Jun. 2021, doi: 10.11591/ijape.v10.i2.pp118-126.
[12] H. Wu, J. Li, and H. Yang, "Research methods for transient stability analysis of power systems under large disturbances," *Energies*, vol. 17, no. 17, p. 4330, Aug. 2024, doi: 10.3390/en17174330.
[13] J. Sun, X. Li, E. Bai, X. Zhang, J. Xu, and P. Yuan, "Analysis of transient voltage characteristics of wind-fire bundling DC external transmission system," in *2022 5th International Conference on Power and Energy Applications (ICPEA)*, Nov. 2022, pp. 51–56, doi: 10.1109/ICPEA56363.2022.10052434.
[14] K. Veerashekar, M. Flick, and M. Luther, "The micro-hybrid method to assess transient stability quantitatively in pooled off-grid microgrids," *International Journal of Electrical Power & Energy Systems*, vol. 117, p. 105727, May 2020, doi: 10.1016/j.ijepes.2019.105727.
[15] Q. H. Wu, Y. Lin, C. Hong, Y. Su, T. Wen, and Y. Liu, "Transient stability analysis of large-scale power systems: a survey," *CSEE Journal of Power and Energy Systems*, vol. 9, no. 4, pp. 1284–1300, 2023, doi: 10.17775/CSEEJPES.2022.07110.
[16] P. Sarajcev, A. Kunac, G. Petrovic, and M. Despalatovic, "Artificial intelligence techniques for power system transient stability assessment," *Energies*, vol. 15, no. 2, p. 507, Jan. 2022, doi: 10.3390/en15020507.
[17] F. Dörfler, M. Chertkov, and F. Bullo, "Synchronization in complex oscillator networks and smart grids," *Proceedings of the National Academy of Sciences*, vol. 110, no. 6, pp. 2005–2010, Feb. 2013, doi: 10.1073/pnas.1212134110.
[18] C. Liu, B. Wang, and K. Sun, "Fast power system simulation using semi-analytical solutions based on Pade approximants," in *2017 IEEE Power & Energy Society General Meeting*, Jul. 2017, pp. 1–5, doi: 10.1109/PESGM.2017.8274297.
[19] H. Stitou, M. A. Atillah, A. Boudaoud, and A. Mounaim, "ETAP software based power flow analysis of 225/60/11KV substation in Tinghir," *E3S Web of Conferences*, vol. 582, p. 01003, Oct. 2024, doi: 10.1051/e3sconf/202458201003.
[20] I. C. Report, "Excitation system models for power system stability studies," *IEEE Transactions on Power Apparatus and Systems*, vol. PAS-100, no. 2, pp. 494–509, Feb. 1981, doi: 10.1109/TPAS.1981.316906.
[21] L. G. W. Roberts, A. R. Champneys, K. R. W. Bell, and M. di Bernardo, "Analytical approximations of critical clearing time for parametric analysis of power system transient stability," *IEEE Journal on Emerging and Selected Topics in Circuits and Systems*, vol. 5, no. 3, pp. 465–476, Sep. 2015, doi: 10.1109/JETCAS.2015.2467111.
[22] L. G. W. Roberts, A. R. Champneys, K. R. W. Bell, and M. Di Bernardo, "Analytical approximations of critical clearing time for parametric analysis of power system transient stability," *IEEE Journal on Emerging and Selected Topics in Circuits and Systems*, vol. 5, no. 3, pp. 465–476, 2015, doi: 10.1109/JETCAS.2015.2467111.
[23] N. Kalloe, J. Bos, J. R. Torres, M. van der Meijden, and P. Palensky, "A fundamental study on the transient stability of power systems with high shares of solar PV plants," *Electricity*, vol. 1, no. 1, pp. 62–86, Nov. 2020, doi: 10.3390/electricity1010005.
[24] A. Agarala, S. S. Bhat, A. Mitra, D. Zychma, and P. Sowa, "Transient stability analysis of a multi-machine power system integrated with renewables," *Energies*, vol. 15, no. 13, p. 4824, Jul. 2022, doi: 10.3390/en15134824.
[25] G. M. Tina, G. Maione, and S. Licciardello, "Evaluation of technical solutions to improve transient stability in power systems with wind power generation," *Energies*, vol. 15, no. 19, p. 7055, Sep. 2022, doi: 10.3390/en15197055.
[26] R. Kamdar, M. Kumar, and G. Agnihotri, "Transient stability analysis and enhancement of IEEE- 9 bus system," *Electrical & Computer Engineering: An International Journal*, vol. 3, no. 2, pp. 41–51, Jun. 2014, doi: 10.14810/ecij.2014.3204.

BIOGRAPHIES OF AUTHORS

Hicham Stitou was born in Azilal, Morocco, in 1989. Graduate teacher in industrial sciences and electrical engineering (SII-IE) in 2018. He is an associate professor of electrical engineering in BTS Center (Higher Technician Diploma Center), SETTAT, Morocco. He received his engineering degree in embedded systems from ENSA of Marrakech in 2015. He is a member of the Engineering and Applied Physics Team (EAPT) at the Superior School of Technology, Sultan Moulay Slimane University, Beni Mellal, Morocco. His research topic is about energy management and optimization in smart grids/microgrids through artificial intelligence solutions. He can be contacted at email: hicham.stitou@usms.ma.

Mohamed Amine Atillah was born in Casablanca, Morocco, in 1991. He has been a professor of engineering sciences and electrical engineering since 2017. Currently, he serves as a professor of electrical engineering at the preparatory classes for higher education schools in Beni Mellal, Morocco. In 2014, he obtained a specialized master's degree in electrical engineering from the Faculty of Sciences Ain Chock, Casablanca. In 2022, he began pursuing his Ph.D. as a member of the Engineering and Applied Physics Team (EAPT) at the Superior School of Technology, Sultan Moulay Slimane University, Beni Mellal, Morocco. His research focuses on the design and implementation of a high-performance optimal control for a photovoltaic conversion chain. He can be contacted at email: mohamedamine.atillah@usms.ma.

Abdelghani Boudaoud was born in Azilal, Morocco, in 1973. He received his Ph.D. in electronics and telecommunications from Hassan 1st University, Settat, Morocco, in 2019. In 2020, he joined the Department of Mechatronics at the Higher School of Technology (EST), Sultan Moulay Slimane University, Beni Mellal, Morocco, as a professor. His current research interests include the hardware design of algorithms applied to information processing and control of industrial systems. He can be contacted at email: abdelghani.boudaoud@usms.ma.

Mounaim Aqil is currently a full professor in the Mechatronics Department at Higher School of Technology, Sultan Moulay Slimane University, Béni-Mellal, Morocco. In 2018, he received his Ph.D. in electrical engineering from Mohammed V University. His current research interests include signal processing, embedded electronic systems, and IoT. He is a member of the Engineering and Applied Physics Team. He can be contacted at email: mounaim.aqil@usms.ma.